Journal of Engineering Science and Technology
Vol. 12, No. 11 (2017) 2866 - 2879
© School of Engineering, Taylor's University

INFLUENCE OF PROCESS PARAMETERS ON THREE BODY ABRASIVE WEAR BEHAVIOUR OF FUNCTIONALLY GRADED ALUMINIUM ALLOY REINFORCED WITH ALUMINA

N. RADHIKA*, M. PRAVEEN, SWARNAVA MUKHERJEE

Department of Mechanical Engineering, Amrita School of Engineering, Coimbatore
Amrita Vishwa Vidyapeetham, Amrita University, India
*Corresponding Author: n_radhika1@cb.amrita.edu

Abstract

The aim of this research is to fabricate functionally graded aluminium composite reinforced with 15 wt% alumina using centrifugal casting technique with dimensions of $Ø_{out}$160 x $Ø_{in}$145 x 150 mm and to investigate its three-body abrasive wear behavior. Hardness tests and microstructural examinations were performed at distances of 2, 8 and 14 mm from outer diameter. Based on hardness test results, wear tests were carried out at a distance of 2 mm from outer diameter and a total of 16 experiments were conducted as per Taguchi's Design of Experiments. The parameters varied were load applied on the specimen (29, 34, 41 and 53 N), sliding speed at the surface of the specimen (75, 100, 125 and 150 rpm) and time of operation (3, 5, 7 and 9 mins) and their influence on the wear rate was analyzed using Analysis of Variance and Signal-to-Noise ratio. The most dominating parameter was found out to be the load applied and subsequently a regression equation was generated. Finally, the worn surfaces were analyzed using Scanning Electron Microscope. The images obtained were used to explain the wear mechanisms and it was found out that increased load caused severe ploughing action on the surface. This indicates that the load applied on the component fabricated with this material is the major factor in determining is life.

Keywords: Taguchi's DOE, Centrifugal casting, Scanning Electron Microscope, Functionally Graded Materials, Wear.

1. Introduction

Industries today require materials to show superior mechanical properties and be lightweight at the same time. Metal Matrix Composites (MMCs) prove to be far

Nomenclatures

Adj SS	Adjacent sum of squares
Adj MS	Adjacent mean of squares
D	Density of alloy, g/cm^3
DF	Degree of freedom
dm	Difference in mass, g
F	Fisher's test
L	Load applied, N
S	Sliding distance, m
Seq SS	Sequential sum of squares
T	Time, min
W	Wear rate, mm^3/Nm

Abbreviations

AMMC	Aluminium Metal Matrix Composite
ANOVA	Analysis of Variance
DOE	Design Of Experiments
FGAMMC	Functionally Graded Aluminium Metal Matrix Composites
FGM	Functionally Graded Material
MMC	Metal Matrix Composite
SEM	Scanning Electron Microscope

more efficient that the conventional monolithic materials [1]. The composition of MMCs can be specified by the metal matrix, reinforcement type and the reinforcement geometry. Most metals have been explored for use in the MMC as the matrix, including Aluminium (Al), Beryllium (Be), Magnesium (Mg), Nickel (Ni) and Titanium (Ti). Materials like Alumina (Al_2O_3), Silicon carbide (SiC) and Boron carbide (B_4C) have been used as reinforcements. Reinforcement shapes like whiskers, fibres and spheroids have been explored. Among all, Aluminium based MMCs (AMMCs) are used and studied most widely because of their superior mechanical properties and low density [2]. Results show that the type of reinforcement in AMMCs significantly affects its wear properties. The result also revealed that particulate reinforcement was most effective in improving the wear properties of the MMCs.

Ceramic particles are preferred as reinforcements due to their stiffness and strength along with lightweight [3]. Research in the field of AMMCs has led to the development of a much more advanced class of composite materials called as Functionally Graded MMCs. Based on the work on two body abrasive wear behaviour, it has been found that the wear rate in AMMCs decreases with increase in sliding speed and increases with increase in normal load [4, 5]. Studies show that using Al_2O_3 or SiC as reinforcements in AMMCs significantly affects the wear properties of the material. Results indicate that the size of the reinforcements also affects the tribological properties [6-8].

Functionally Graded MMCs contain reinforcement particles whose concentration varies continuously from inner to outer section of composite specimen and thus providing a controlled non-uniform microstructure with continuously varying properties [9]. These types of materials are usually used when

the application requires the part to be hard on the surface and strong in the inner part. This characteristic is usually not found in monolithic counter parts of the Functionally Graded Materials (FGMs) [10]. Composites with aluminium matrix are preferred due to their mechanical properties and low density. FGMs with aluminium metal matrix are called as Functionally Graded Aluminium Metal Matrix Composites (FGAMMCs). A number of ways have been proposed for the synthesis of FGMs such as simultaneous combustion and compaction, low vacuum vapour deposition, powder metallurgy and centrifugal casting. In the case of process of simultaneous combustion and compaction, the materials are initially taken as powders and then compacted inside a heated chamber [11]. Another process used for the purpose is a low vacuum vapour deposition process [12]. Helium jets in combination with electron beams are used for spray deposition on the substrate surface. In powder metallurgy, different samples with different layers of FGMs are compacted using steel die and punch at sintered temperature [13].

Another effective way to produce FGMs is centrifugal casting [14]. In this process, molten metal with the reinforcement particles is poured into a rotating die and made to solidify inside it. Among the processes explored, it was found out that centrifugal casting is the most widely used process to produce FGMs [15, 16]. The parameters that can be varied in the process of centrifugal casting are the speed of rotation, temperature of the die and the temperature of molten metal. It has been reported that the speed of rotation decides the gradient of the volume fraction of reinforcement particles. Also, the temperature of the mould decides the surface properties of the obtained cast [17]. There are several optimisation methods like central composite design, response surface methodology, Taguchi's method etc., available in order to perform an experiment [18, 19]. Taguchi's Design of Experiments (DOE) is found to be an effective tool in reducing the total number of experiments performed without compromising on the end result [20, 21].

Since FGAMMCs are light and their properties can be changed along the length, they exhibit excellent tribological properties. Due to this reason, FGAMMCs have great applications in aerospace and automotive industries [22, 23]. Based on the literature survey, it was identified that not much research has been done on three-body abrasive wear properties of FGMs. Thus, the current work deals with fabrication of FGAMMC reinforced with alumina and optimisation of its abrasive wear variables using Taguchi's DOE.

2. Material Selection

The material selected for fabrication of FGAMMC was Al-Si5Cu3 (density 2.79 g/cm^3) since it is widely used for manufacturing engine blocks, cylinder heads, crank cases and high performance ballistic armours. They also have a huge scope in the aerospace industry due to high thermal property gradients that can be achieved through them. Al_2O_3 of size 10 µm with a density of 3.95 g/cm^3 and 15 wt% was taken as the reinforcement due to its improved wear resistance and hardness properties. The elemental composition of the alloy is shown in Table 1.

Table 1. Elemental composition of Al-Si5Cu3 alloy.

Element	Si	Fe	Cu	Mn	Mg	Ni	Zn	Ti	Al
Wt%	4.3	0.5	2.2	0.2	0.16	0.039	0.3	0.028	92.273

3. Synthesis of Functionally Graded Composite

Initially, the alloy Al-Si5Cu3 was taken in a crucible made of graphite and was kept in an electrical resistance furnace (Fig. 1). The inside of the chamber was maintained at inert condition by supplying argon gas. This was done in order to prevent any sort of redox reaction so as to make the casting free of defects. After the alloy had melted at around 760 ºC, the preheated Al_2O_3 reinforcement particles (300 ºC) were gradually added to it through the hopper setup in the furnace. A mechanically operated stirrer was rotated at 300 rpm in order to uniformly disperse the reinforcement particles within the molten metal. The crucible was then taken out of the furnace and the molten metal was poured into the metallic die maintained at 350 ºC of the horizontal centrifugal casting machine (Fig. 2). The die has an inner diameter of 160 mm and a length of 150 mm which rotates at a speed of 1250 rpm. A belt and pulley arrangement was used to transmit power between the motor and the die. It was rotated till the solidification was complete. The hollow cylindrical cast component was then removed from the die. The dimensions of the obtained cast were measured to have an outer diameter of 160 mm, a thickness of 15 mm and length of 150 mm.

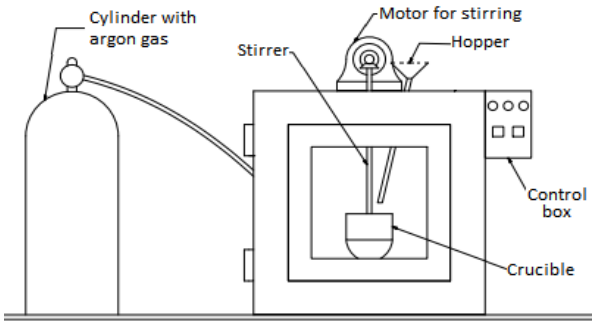

Fig. 1. Furnace with stirrer setup.

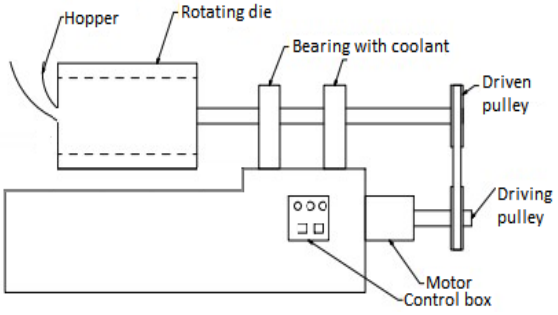

Fig. 2. Centrifugal casting machine.

4. Experiments Performed

Different tests were performed in order to evaluate the hardness, microstructure, abrasive wear and wear surface topology.

4.1. Hardness test

The specimens were tested for their hardness at three distances (2, 8 and 14 mm) measured from outer diameter of the cast. This test was done in order to analyze the effect of particle density on the hardness. The hardness test was performed using Vicker's hardness tester according to ASTM E-384 test procedure. Before the experiment, the surface of specimen was made flat so that proper indentation on the specimen was obtained. The indentation was done by a diamond indenter which was in the shape of a pyramid. A load of 500 g was applied which in turn developed an indentation area and was measured by a microscope. Based on the indentation area, the hardness value was then estimated.

4.2. Microstructure examination

The specimens used for observing the microstructure were prepared and polished. The initial polishing was done by using emery paper in the order of grits 1/0, 2/0, 3/0 and 4/0 respectively and final buffing was done using liquid alumina to get a mirror like finish. Keller's reagent was used as an etchant to observe features. The microstructure was observed using Zeiss Axiovert CA 25 Optical Inverted Microscope. The microstructure was observed at a distance of 2, 8 and 14 mm from the outer diameter of the cast in order to study the variation of reinforcement particles.

4.3. Three-body abrasive wear test

The cast component was cut to specimens of size (75 x 25 x 2.5 mm) and was utilized for performing the test in the sequential order as per Taguchi's DOE technique. The dry abrasion wear tester was used to do the abrasion test as per ASTM (G-65) standard of composite specimens. The tester consists of chlorobutyl wheel of 228 mm diameter which can rotate at a preset rpm and acts as a counter face. Above the chlorobutyl wheel, a hopper was present from where an abrasive was supplied for conducting the experiment. The abrasive used for conducting the experiment was silica sand grade AFS 55/70 and the flow rate of silica sand was maintained at 350 g/min. The tester also consists of a lever whose one end was connected to a loading pan where loads were applied on the specimen while at the other end, the specimen was fixed. Equation 1 gives the value of the applied load (L) on the specimen:

$$L = 9.81(0.24Wt + 2.4) \quad (1)$$

Here 0.24 and 2.4 are the setup parameters and '*Wt'* is the applied weight in kg. The initial mass of the specimen was noted by using a physical balance whose accuracy is 0.1 mg. The specimen was then fixed to the tester and the experiment was conducted and then, final weight of specimen was found. Before the start of next experiment, dressing operation was done on the wheel to ensure that there are no particles along the circumference of the wheel. Equation 2 gives the wear rate (W) of the given specimen (mm^3/Nm), where dm is the difference in mass of the sample before and after the experiment (g), d is the alloy density (g/mm^3), L is the applied load (N) and S is the sliding distance in m.

$$W = dm/dLS \quad (2)$$

4.4. Taguchi's design of experiments

Taguchi's DOE was used to measure the effect of various parameters and their combinations by performing least number of experiments and to know their effect on a particular behavior. It was also used to determine the optimum condition of the parameters which could give better results. The parameters used for performing the abrasive wear behavior of the FGM were applied load, sliding speed and the time for which the testing was done in the dry abrasion tester. Based on the parameters and the levels shown in Table 2, a full factorial L_{16} array was produced using the Taguchi's DOE to study the wear behavior.

Table 2. Parameters and levels of wear

S. No.	Load (N)	Speed (rpm)	Operation time (min)
1	29	75	3
2	34	100	5
3	41	125	7
4	53	150	9

5. Results and Discussion

The tests for hardness, microstructure examination, abrasive wear behavior of material using Taguchi's DOE and ANOVA and the Scanning Electron Microscope (SEM) analysis of the components after testing are discussed in detail below.

5.1. Hardness evaluation

The hardness of the FGAMMC reinforced with Al_2O_3 at three different distances from outer diameter of the material is shown in Table 3. It is observed that the hardness value continuously decreases radially inward from outer diameter. This is due to segregation of higher number of reinforcement particles along outer diameter. When the material was fabricated by centrifugal casting, the heavier particles tend to move towards outer diameter due to centrifugal force. This centrifugal force is proportional to the square of angular speed. Due to this reason, the reinforcement particles are forced radially in the outward direction and thus leading to a higher amount of reinforcement particles on the outer diameter. This gradient of particles is the reason for the observed trend in hardness values along the radial direction.

Table 3. Results of hardness test.

Distance from outer diameter (mm)	2	8	14
Hardness Value (HV)	176	128	92

5.2. Microstructure evaluation

Figures 3(a), (b) and (c) represent the microstructure at 2, 8 and 14 mm respectively from the outer diameter along the radial direction. The small granules observed are the Al_2O_3 reinforcement particles. It is observed that the number of reinforcement particles decreases as the distance from the outer diameter increases. This is attributed to the centrifugal force induced by the rotating die during fabrication. The presence of comparable number of particles at the centre, Fig. 3(b) and inner

portions, Fig. 3(c) is attributed to the air bubbles generated due to the impurities in the cast. These bubbles carry the reinforcement particles within them towards the centre due to the buoyancy force. Another reason for this could probably be due to the speed of rotation of the die which induces less amount of centrifugal force on the particles. Figure 4 shows the SEM image of Al_2O_3 reinforcement particles used. As per the hardness and microstructure evaluation, it is observed that the outer diameter of the cast is the hardest and has Al_2O_3 particle rich region. Thus, further tests had been done on outer diameter of the cast.

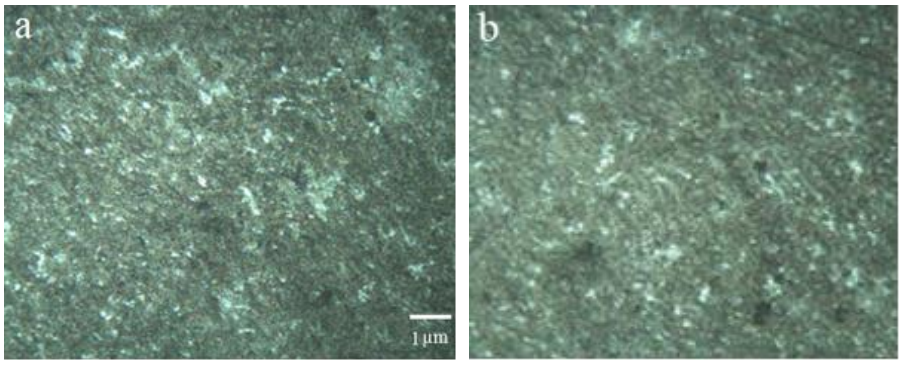

(a) 2 mm from outer diameter. **(b) 8 mm from outer diameter.**

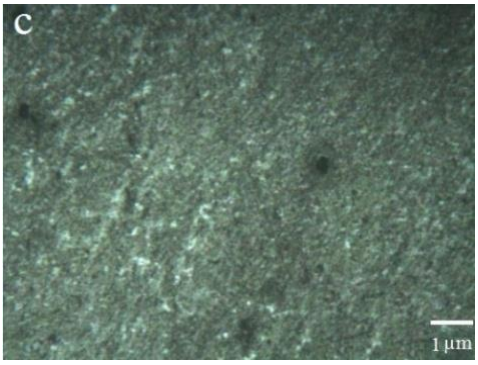

(c) 14 mm from outer diameter.

Fig. 3. Microstructural examination of composite.

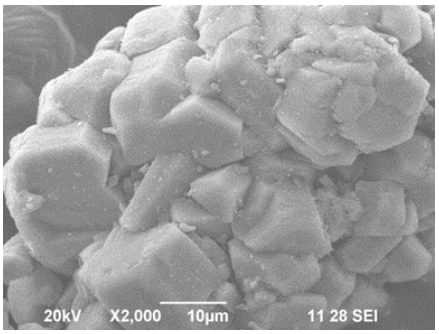

Fig. 4. SEM image of Al_2O_3 reinforcement particles.

5.3. Evaluation of three body abrasive wear

The abrasion tests were obtained by varying parameters like speed, load and time of contact as per the L_{16} array. The results are tabulated in Table 4. The mean plot of the wear rate was also generated and is shown in Fig. 5. These plots show the trend with which the wear rate varies about the mean wear rate, with a particular parameter.

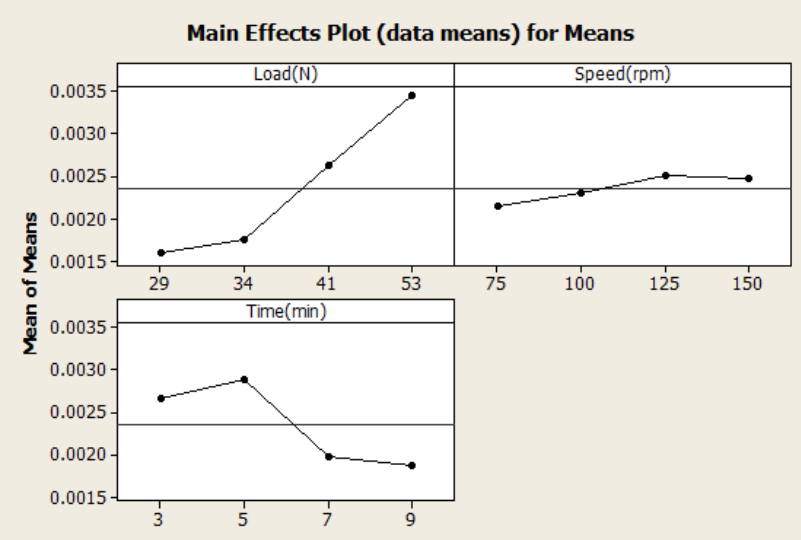

Fig. 5. Plot of mean of means.

Table 4. Results of wear test.

Exp. No.	Load (N)	Speed (rpm)	Time (min)	Wear rate (mm^3/Nm)
1	29	75	3	0.002139
2	29	100	5	0.002340
3	29	125	7	0.000989
4	29	150	9	0.000934
5	34	75	5	0.001726
6	34	100	3	0.001684
7	34	125	9	0.001755
8	34	150	7	0.001861
9	41	75	7	0.002331
10	41	100	9	0.002452
11	41	125	3	0.002738
12	41	150	5	0.002982
13	53	75	9	0.002395
14	53	100	7	0.002741
15	53	125	5	0.004558

16	53	150	3	0.004088

5.3.1. Effect of load

It is observed from Fig. 5 that the wear rate increases as the load on the sample increases. It is seen that the wear rate does not increase much for small loads. At smaller loads, the silica sand particles tend to fall freely as they are partially pressed against the surface. There is only rolling motion of the silica sand particles against the surface. This results in only minor scratches on the surface and hence low wear rate. As the load is increased, the sand grains are pressed harder against the surface. These results in both rolling ad rubbing of sand grains against the surface causing deeper penetration of the sand particles leading to ploughing of the material. Due to this increased compression of the sand grains, the temperature rises and leads to the penetration and eventually deposition of these particles into the rubber wheel. This, in addition to the ploughing action, results in higher wear rate at increased loads and similar trend is being observed [24].

5.3.2. Effect of time

The wear rate is found to decrease with the increase in abrasion time and is also evident from Fig. 5. The initial increase in wear rate is attributed to the protruding reinforcement particles on the surface of the specimen. This leads to a non-uniform contact between the wheel and the specimen resulting in abrasion of these protrusions. But as the abrasion time increases, the surface becomes smoothened by the wheel leading to decreased wear rate and similar phenomena is reported [25].

5.3.3. Effect of speed

It is observed that the wear rate does not vary much with the sliding speed (Fig. 5). This is attributed to the hardness of the surface and the uniformity of the wheel; it does not cause much of a fatigue loading on the hard surface of the specimen. This is the reason for minimum variation of wear rate with the sliding speed. Although, the variation is small, there is still an increasing trend that is observed. As the speed increases, the work done by the friction force also increases. This is the reason for the increase in wear rate with the speed and similar trend is being observed [14].

5.3.4. S/N ratio analysis

The Signal-to-Noise (S/N) ratio analysis is made in order to narrow down the parameter which affects the wear rate the most. Table 5 shows the response table and the delta value indicates the influence of that particular parameter on the wear rate. It is basically the difference of the maxima and minima of a particular parameter. Higher the delta value, higher is its contribution on the wear rate. It is observed from Table 5, that the most contributing parameter on the wear rate is load succeeded by time of contact and sliding speed.

Figure 6 shows the mean effect plot for S/N ratio of wear rate. Based on the plot, it is observed that the optimum condition for operation of specimen is found to be at a load of 29 N, sliding speed of 75 rpm and a time of operation of 9 minutes.

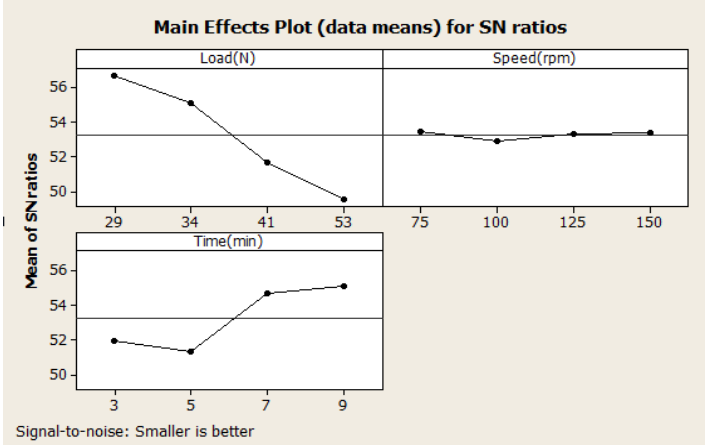

Fig. 6. Mean effect plot for S/N Ratio - Wear rate.

Table 5. Response table for S/N ratio.

Level	Load (N)	Speed (rpm)	Time (min)
1	56.67	52.8	51.97
2	55.1	53.3	51.3
3	51.65	53.3	54.65
4	49.56	53.4	55.08
Delta	7.11	0.5	3.7
Rank	1	3	2

5.3.5. Analysis of variance (ANOVA)

Analysis of variance **(**ANOVA) was applied for the obtained results to measure the influence on wear rate by each parameter. Here the analysis is done in order to know the contribution of load, sliding speed and time of contact on the wear rate of the specimen. The analysis was performed for a 95% confidence level and 5% significance level. The values of the interaction parameters 'P' below 0.05 indicate the influence of that particular parameter on the wear rate is significant. A value above 0.05 indicates that the contribution of that particular parameter is not very significant. The last column in Table 6 shows the percentage contribution (P %) of each parameter. It is seen that the load has a contribution of 63.31% followed by time, which has a contribution of 21.58% followed by sliding speed, which has a contribution of 2.158%. This reassures the results obtained from the S/N ratio analysis.

5.3.6. Regression equation analysis

Equation 3 shows the regression obtained through ANOVA

$$W = -0.000373 + 0.000081(L) + 0.000005(S) - 0.000163(T) \quad (3)$$

where, W = Wear rate (mm^3/Nm); L = Load (N); S = Sliding speed (rpm); T = Time of contact (min).

The regression equation was obtained based on the percentage contribution of each of the factors. The positive sign for the load and speed term in the equation shows that the wear rate increases with an increase in these factors. The negative

sign in the time term shows that the wear rate decreases with an increase in this factor. The equation was then tested for conditions other than the levels chosen from the L_{16} array to check for it accuracy. Table 7 shows the conditions that were tested and the wear rates obtained experimentally as well as from the regression equation. It is observed that the results of regression equation agree well with the experimental values with a maximum error of 6.59%.

Table 6. Analysis of variance for wear rate.

Source	DF	Seq SS	Adj SS	Adj MS	F	P	P%
L (N)	3	0.88E-05	0.88E-05	0. 29E-05	9.58	0.011	63.31
S (rpm)	3	0.03E-05	0.03E-05	0. 01E-05	0.36	0.785	2.158
T (min)	3	0.30E-05	0.30E-05	0. 10E-05	3.30	0.099	21.58
Error	6	0.18E-05	0.18E-05	0. 03E-05			12.95
Total	15	0.14E-04					

Table 7. Regression equation analysis.

S. No.	L (N)	S (rpm)	T (min)	Reg. wear rate (mm^3/Nm)	Exp. wear rate (mm^3/Nm)	Error (%)
1	32	90	4	0.002017	0.001884	6.59
2	38	115	6	0.002302	0.002251	2.26
3	46	135	8	0.002724	0.002623	3.85

5.4. Scanning electron microscope analysis

The worn-out surfaces observed using SEM analysis is shown in Fig. 7. The cases taken for SEM study can explain the wear behavior of the composite in a complete manner. Figures 7(a) and (b) show the effect of load on the sample as it contributes the most to the wear rate. It is seen that the speed of the abrasive wheel is different in the two cases, Figs. 7(a) and (b), but it does not affect the wear behavior much as its contribution is less than 3%. It is observed that for a load of 41 N, Fig. 7(a), the surface of the specimen does not show prominent long scratches. This is attributed to the fact that the load is not sufficient enough to push the silica sand grains into the surface to cause ploughing. In the case of 51 N, Fig. 7(b), long and deep scratched are observed. This is because the higher load pushes the silica sand particles into the surface and causes a deep ploughing action resulting in such a worn surface, similar mechanism is observed by Das et al [24].

Figures 7(c) and (d) show the effect of time on the wear behavior as it is the second most influential factor on the wear rate. It is seen that the speed for both the cases are different but the effect of speed on the wear rate is negligible. It is observed that the worm surface for a longer period of application of load, Fig. 7(d) is smoother than that of smaller period of application of load, Fig. 7(c). For smaller abrasion time, the reinforcement particles protruding on the surface are worn out. But as the abrasion time increases, the surface becomes smoothened due to the prolonged contact of the rubber wheel resulting in lower wear rate [25].

According to the S/N ratio analysis, the optimum conditions were found out to be 29 N, 75 rpm and 9 mins of operation. An experiment with these conditions was performed and a SEM image of the resulting worn surface is shown in Fig. 8. The scratches were found to be minimal which indicates minimal wear rate and is similar to the results obtained by another researcher [26].

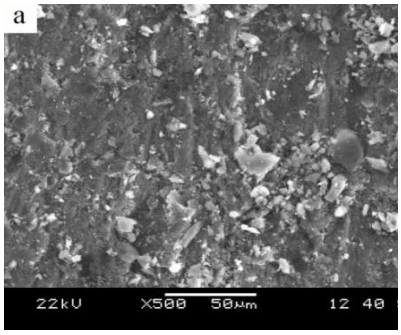

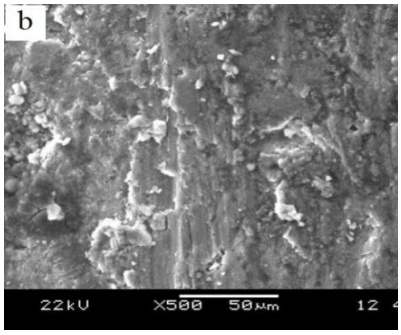

(a) T= 9 mins, S = 100 rpm, L = 41 N. **(b) T=9 mins, S=75 rpm, L = 53 N.**

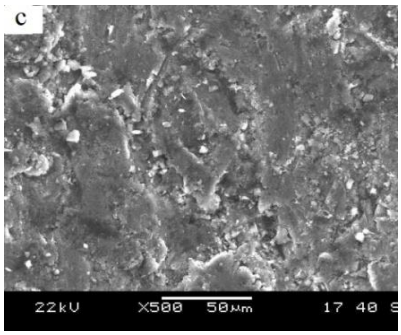

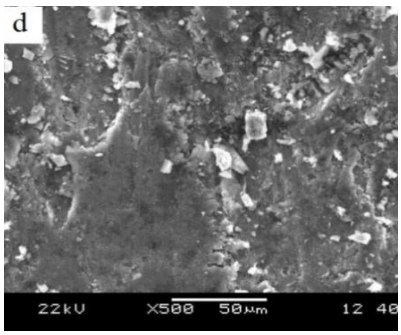

(c) T=5 mins, S =75 rpm, L=34 N. **d) T =9 mins, S=150 rpm, L=34N.**

Fig. 7. Results of SEM examination of worn surfaces.

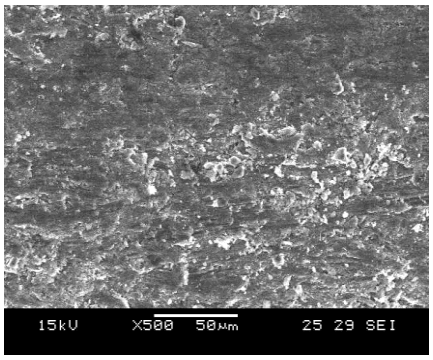

Fig. 8. SEM image of worn surface at optimum condition.

6. Conclusion

Functionally graded aluminium metal matrix composite containing Al_2O_3 reinforcement particles is successfully fabricated using the process of centrifugal casting. It is inferred from hardness and microstructural examinations that, the number of reinforcement particles is maximum at a distance of 2 mm from the outer diameter and decreases along the radial direction. Wear tests performed at a

distance of 2 mm from the outer diameter revealed that the influence of load on wear is maximum succeeded by the time of operation and sliding speed. This result has been confirmed both by the S/N ratio and the ANOVA of the mean wear rates. It is confirmed from the SEM analysis that the reinforcement particles prevent the occurrence of wear to a great extent. Thus, FGAMMC with Al_2O_3 reinforcement particles are suitable for industrial applications requiring high wear resistance. They can primarily be used for producing components like brake drums which require a hard surface on the diameter.

References

1. Meena, K.L.; Manna, A.; Banwait, S.S.; and Jaswanti. (2013). An analysis of mechanical properties of the developed Al/SiC-MMC's. *American Journal of Mechanical Engineering*, 1(1), 14-19.
2. Hunt, W.; and Herling, D.R. (2004). Aluminum metal matrix composites. *Advanced Materials and Processes*, 162(2), 39-44.
3. Ibrahim, I.A.; Mohamed, F.A.; and Lavernia, E.J. (1991). Particulate reinforced metal matrix composites - A review. *Journal of Material Sciences*, 26(5), 1137-1156.
4. Melgarejo, Z.H.; Suárez, O.M.; and Sridharan, K. (2006). Wear resistance of a functionally-graded aluminum matrix composite. *Scripta Materialia*, 55(1), 95-98.
5. Nai, S.M.L.; and Gupta, M. (2002). Influence of stirring speed on the synthesis of Al/SiC based functionally gradient materials. *Composite Structures*, 57(1-4), 227-233.
6. Zhang, X.H.; Han, J.C.; Du, S.Y.; and Wood, J.V. (2000). Microstructure and mechanical properties of TiC-Ni functionally graded materials by simultaneous combustion synthesis and compaction. *Journal of Materials Science*, 35(8), 1925-1930.
7. Groves, J.F.; and Wadley, H.N.G. (1997). Functionally graded materials synthesis-via low vacuum directed vapor deposition. *Composites Part B*, 28(1-2), 57-69.
8. Radhika, N.; and Raghu, R. (2015). Parametric study of dry sliding wear behavior of functionally graded Al LM25/Si_3N_4 composite by response surface methodology. *Advanced Composite Letters*, 24(6), 130-136.
9. Rajan, T.P.D.; Pillai, R.M.; and Pai, B.C. (2010). Characterization of centrifugal cast functionally graded aluminum-silicon carbide metal matrix composites. *Material Characterisation*, 61(10), 923-928.
10. Watanabe, Y.; Kawamoto, A.; and Matsuda, K. (2002). Particle size distributions in functionally graded materials fabricated by the centrifugal solid-particle method. *Composites Science and Technology*, 62(6), 881-888.
11. Panda, E.; Mehrotra, S.P.; and Mazumdar, D. (2006). Mathematical modeling of particle segregation during centrifugal casting of metal matrix composites. *Metallurgical and Materials Transactions A*, 37(5), 1675-1687.
12. Bertolino, N.; Monagheddu, M.; Tacca, A.; Giuliani, P.; Zanotti, C.; Maglia, F.; and AnselmiTamburini, U. (2003). Self-propagating high-temperature

synthesis of functionally graded materials as thermal protection systems for high-temperature applications. *Journal of Material Research*, 18(2), 448-455.

13. Nemat-Alla, M.M.; Ata, M.H.; Bayoumi, M.R.; and Khair-Eldeen, W. (2011). Powder metallurgical fabrication and microstructural investigations of aluminum/steel functionally graded material. *Materials Sciences and Applications, 2*(12), 1708.
14. Agarwal, G.; Patnaik, A.; and Sharma, R.K. (2012). Parametric optimization of three-body abrasive wear behavior of bidirectional and short kevlar fiber reinforced epoxy composites. *International Journal of Engineering Research and Applications*, 2(6), 1148-1167.
15. Venkataraman, B.; and Sundararajan, G. (2000). Correlation between the characteristics of the mechanically mixed layer and wear behavior of aluminium Al-7075 alloy and Al-MMCs. *Wear*, 245(1-2), 22-38.
16. Baradeswaran, A.; ElayaPerumal, A. (2014). Study on mechanical and wear properties of Al7075/Al_2O_3/graphite hybrid composites. *Composites*, 56(1), 464-471.
17. Israa, A.K. (2013). Studying the effect of reinforcing by SiC_p on the dry sliding wear behavior and mechanical properties of Al-4% Cu matrix alloy. *Journal of Engineering Sciences*, 6(2), 139-153.
18. Asghar, A.; Abdul Raman, A.A.; and Daud, W.M.A.W. (2014). A comparison of central composite design and Taguchi method for optimizing Fenton process. *Scientific World Journal*, 1-14.
19. Radhika, N.; and Raghu, R. (2015). Dry sliding wear behaviour of aluminium Al-Si12Cu/TiB_2 metal matrix composite using response surface methodology. *Tribology Letters*, 59 (2), 1-9.
20. BallalYuvaraj, P.; Inamdar, K.H.; and Patil, P.V. (2012). Application of Taguchi method for Design of Experiments in turning grey cast iron. *International journal of Engineering Research and Applications*, 2(3), 1391-1397.
21. Radhika, N.; and Subramanian, R. (2013). Wear behavior of aluminium/alumina/graphite hybrid metal matrix composites using Taguchi's techniques. *Industrial Lubrication and Tribology*, 65(3), 166-174.
22. Singh, M.; Mondal, D.P.; and Das, S. (2006). Abrasive wear response of aluminium alloy-sillimanite particle reinforced composite under low stress condition. *Material Sciences and Engineering*, 419(1-2), 59-68.
23. Das, S.; Mondal, D.P.; Sawla, S.; and Ramakrishnan, N. (2008). Synergic effect of reinforcement and heat treatment on the two body abrasive wear of an Al-Si alloy under varying loads and abrasive sizes. *Wear*, 264(1-2), 47-59.
24. Mondal, D.P.; and Das, S. (2006). High stress abrasive wear behavior of aluminium hard particle composites: Effect of experimental parameters, particle size and volume fraction. *Tribology International*, 39(6), 470-478.
25. Canakci, A. (2011). Microstructure and abrasive wear behavior of B_4C particle reinforced 2014 Al matrix composites. *Journal of Materials Science*, 46(8), 2805-2813.
26. Priyanka Muddamsetty, L.V.; and Radhika, N.(2016). Effect of heat treatment on the wear behavior of functionally graded LM13/B_4C composite. *Tribology in Industry*, 38 (1), 108-114.